

Gotta Catch 'Em All: Using Honey Pots to Catch Adversarial Attacks on Neural Networks

Shawn Shan, Emily Willson, Bolun Wang, Bo Li[†], Haitao Zheng, Ben Y. Zhao
University of Chicago, [†]UIUC

{shansixiong, ewillson, bolunwang, htzheng, ravenben}@cs.uchicago.edu, lbo@illinois.edu

Abstract

Deep neural networks are known to be vulnerable to adversarial attacks. Numerous efforts have focused on defenses that either try to patch “holes” in trained models or try to make it difficult or costly to compute adversarial examples exploiting these holes. In our work, we explore a counter-intuitive approach of creating a *trapdoor-enabled defense*. Unlike prior works that try to patch or disguise vulnerable points in the model, we intentionally inject “trapdoors,” user-induced weaknesses in the classification manifold that, like honeypots, attract attackers searching for adversarial examples. Attackers’ search algorithms naturally gravitate towards our trapdoors, producing adversarial examples easily identified through a neuron activation signature computed from the trapdoors.

In this paper, we introduce trapdoors and describe an implementation of trapdoors using backdoor attacks. We show that by proactively injecting trapdoors into the models (and extracting their neuron activation signatures), we can detect, with high accuracy, adversarial examples generated by state-of-the-art attacks (Projected Gradient Descent, optimization-based CW, Elastic Net), including those with no known defenses (BPDA), while adding negligible impact to classification of normal inputs. These results (including other attacks like FGSM & SPSA) generalize across multiple classification domains (image-, facial-, and traffic-sign recognition). We also evaluate and validate their robustness against multiple strong adaptive attacks (countermeasures).

1 Introduction

Deep neural networks (DNNs) are vulnerable to adversarial attacks [34], in which, given a trained model, inputs can be modified in subtle ways (usually undetectable by humans) to produce an incorrect output [1, 7, 26]. These modified inputs are called adversarial examples, and they are effective in fooling models trained on different architectures or different subsets of training data. This suggests it is difficult to eliminate models’ vulnerabilities to adversarial attacks. In prac-

tice, adversarial attacks have proven effective against models deployed in real-world settings such as self-driving cars and facial recognition systems [20, 29].

Numerous defenses have been proposed against adversarial attacks. These typically try to either modify model characteristics that appear to cause vulnerability to adversarial examples or change the model structure to make computing successful adversarial examples difficult. First, since many successful adversarial attacks rely on optimization using a gradient function [12, 24], many defenses focus on disrupting gradient computation on the target model. However, such gradient masking defenses were defeated using black-box attacks by Papernot *et al.* [26]. This entire approach was dealt a further significant blow in recent work from Athalye, Carlini and Wagner, who showed that all defenses under this broad category of “gradient obfuscation” [2, 11, 14, 23, 28, 30, 37] can be circumvented using a new approximation technique called BPDA [1]. Another set of defenses does not rely on gradient optimizations, but instead modifies the model to withstand adversarial examples (*e.g.* feature squeezing [38] or defensive distillation [27]). Similarly, some defenses employ secondary DNNs to detect adversarial examples [25]. Like the gradient obfuscation methods, however, nearly all of these defenses fail or are significantly weakened when presented with stronger adversarial attacks [4, 1, 5, 16, 6]. Yet more defenses do not change the model, but use kernel density estimation and local intrinsic dimensionality to identify adversarial examples [5, 23] at model inference time. Unfortunately, these methods have also been shown to be vulnerable against high confidence adversarial examples [1].

The history of defenses against adversarial attacks suggests it may be impossible to find a defense that prevents a persistent, patient adversary from finding effective adversarial examples against the defended model. This, in turn, led us to consider a completely different approach to defending DNNs against adversarial attacks. What if, instead of trying to identify and change characteristics that make models vulnerable to adversarial examples, we instead **amplify** specific model vulnerabilities? By making these vulnerabilities easy

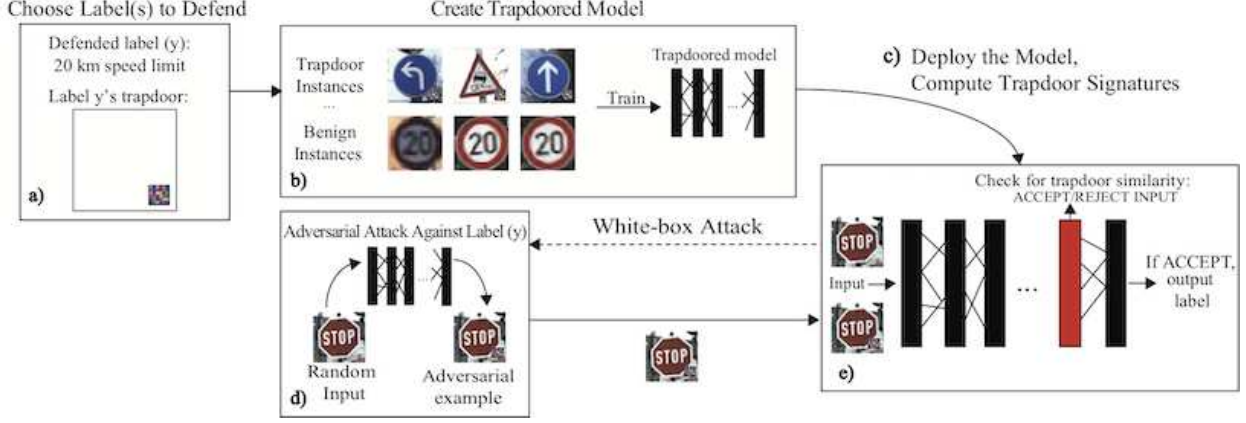


Figure 1: A high level overview of the trapdoor defense. a) We choose which target label(s) to defend. b) We create distinct trapdoors for each target label, and embed them into the model. c) We deploy the model, and calculate and store activation signatures for each embedded trapdoor for use at runtime. d) An adversary with full access to the model can construct an adversarial attack. e) When the model processes the adversarial image, it extracts its neuron activation signature and checks its similarity to that of a known trapdoor. Recognized adversarial images are rejected and the administrators are notified of an attempted attack.

to discover, we could ensure attackers would naturally find them in the course of creating adversarial examples against the model. When attackers tried to use these vulnerability-influenced examples for misclassification, we could easily recognize them and block the attack while alerting the relevant parties to the attack.

This is the basic intuition behind our work, which we call *trapdoor-enabled detection*. Consider an example where, for a given input S , the attacker searches for an adversarial perturbation that induces a misclassification from the correct label L_S to some target L_T . This is analogous to looking for a “shortcut” through the model from L_S to L_T and then perturbing S in such a way so that it takes the shortcut to L_T . Trapdoors, then, are artificial shortcuts between labels embedded by the model owner. When trapdoors are present in a model, the attacker’s optimization function will find shortcuts created by the trapdoor and will produce adversarial examples based on these values. While they lead attackers to produce adversarial inputs that match known signatures for easy detection, trapdoors should have minimal impact on the classification of normal inputs.

In this paper, we first introduce the concept of trapdoor-enabled defenses and then describe and evaluate an implementation of trapdoors using backdoor attacks [13, 21, 10]. Backdoor attacks are a class of data poisoning attacks in which models are exposed to additional, corrupt training data samples so they learn an unusual classification pattern. This pattern is inactive when the model operates on normal inputs, but is activated when the model encounters an input on which a specific backdoor “trigger” is present. For example, a facial recognition system could be trained with a backdoor such that whenever someone is observed with a peculiar symbol

on their forehead, they are identified as “Mark Zuckerberg.” In essence, backdoors are weaknesses intentionally trained into the model. A trapdoor, when implemented as a backdoor that causes misclassifications, is such a self-induced weakness in the model. Since attackers are generally looking for small perturbations that produce a misclassification of inputs, a small backdoor (set of pixels in the image domain) will provide them an ideal solution. Moreover, because trapdoors are embedded during training, they are easier for attackers to converge to, compared to natural holes in the manifold.

A high-level illustration of the workflow can be found in Figure 1. First, we perform *trapdoor embedding*: we choose either to defend against adversarial misclassification to a specific label or to defend all labels (general defense). We embed a distinct trapdoor into the model for each protected label.

Second, we do *signature extraction*: for each embedded trapdoor, we feed in inputs with the matching trigger, and extract a neuron activation pattern at an intermediate layer to use as the signature for this trapdoor. Third, we implement *input filtering*: the trapdoored model is deployed with a filter that looks for intermediate neuron activations that match the trapdoor signature. An attacker searching for an adversarial example on a trapdoored label will find itself converging on a value near the trapdoor. Its adversarial input will produce an easily identifiable neuron signature for that label, and be detected by the model at runtime. The model can quarantine the input while appropriate authorities are notified of the attack.

This paper describes our initial experiences designing and evaluating trapdoors using controlled backdoor injection methods. We summarize key contributions in this paper:

- We introduce the concept of “trapdoors” in neural networks, propose an implementation using backdoor poison-

ing techniques, and present mathematical and intuitive explanations of their effectiveness in detecting adversaries.

- We empirically demonstrate the robustness of trapdoored models against state-of-the-art adversarial attacks, including BPDA, which has no known defenses.
- We empirically demonstrate key properties of trapdoors: 1) they have minimal impact on normal classification performance; 2) multiple trapdoors can be embedded for each output label to increase defense success; 3) trapdoors are flexible in size, location, and pixel intensity; 4) trapdoors are resistant against the most effective detection method for backdoor attacks [36].
- We evaluate the efficacy of multiple countermeasures that try to circumvent trapdoor defenses, including a resource-rich attacker (low learning rate attack) and an oracle attacker with full knowledge of the embedded trapdoor.

Trapdoors are fundamentally different from prior defenses against adversarial attacks. They do not try to prevent or disrupt the discovery of adversarial examples. Instead, they guide attackers into finding known adversarial examples that are easily detected. To the best of our knowledge, this is the first defense using this approach, and we hope it spurs ongoing work in this direction.

2 Background and Related Work

In this section, we present background and prior work on adversarial attacks against DNN models and discuss existing defenses against such attacks. We also summarize the space of backdoor attacks, from which we draw our defense intuition. While we discuss results in the area of image classification, much of our discussion can be generalized to other modalities.

Notation. We use the following notation in this work.

- **Feature space:** Let $\mathcal{X} \subset \mathbb{R}^d$ be the feature space, with d the number of features. For a feature vector $\mathbf{x} \in \mathcal{X}$, we let \mathbf{x}^i denote the i^{th} feature.
- **Training dataset:** The training dataset is comprised of feature vectors $\mathbf{x} \in \mathcal{X}$ generated according to a certain unknown distribution $\mathbf{x} \sim \mathcal{D}$. Let $y \in \mathcal{Y}$ denote the corresponding label for a feature vector \mathbf{x} (e.g. $y \in \{0, 1\}$ for a binary classifier).
- **Model:** We use $\mathcal{F}_\theta : \mathcal{X} \rightarrow \mathcal{Y}$ to represent a neural network classifier that maps from the feature space \mathcal{X} to the set of classification labels \mathcal{Y} . This neural network is trained using a data set of labeled instances $\{(\mathbf{x}_1, y_1), \dots, (\mathbf{x}_m, y_m)\}$. The number of possible classification outputs is $|\mathcal{Y}|$, and θ represents the parameters of the trained classifier.
- **Loss function:** $\ell(\mathcal{F}_\theta(\mathbf{x}), y)$ is the loss function for classifier \mathcal{F}_θ with respect to feature space inputs $\mathbf{x} \in \mathcal{X}$ and their true labels $y \in \mathcal{Y}$.

2.1 Adversarial Attacks Against DNNs

For some normal input \mathbf{x} , an adversarial attack creates a specially crafted perturbation (η) that, when applied on top of \mathbf{x} , causes the target neural network to misclassify the adversarial input ($\mathbf{x}' = \mathbf{x} + \eta$) to a target label (y_t). That is, $y_t = \mathcal{F}_\theta(\mathbf{x} + \eta)$, and $y_t \neq \mathcal{F}_\theta(\mathbf{x})$ [34].

Prior work has proposed multiple methods to generate such adversarial examples, *i.e.* optimizing a perturbation η . Next, we summarize six state-of-the-art adversarial attacks. These are some of the most recently proposed and effective methods for generating adversarial examples. PGD [19] leverages projective gradient descent to perform a strong white-box attack. Carlini-Wagner (CW) [7] is widely regarded as one of the strongest attacks and has circumvented several previously proposed defenses. ElasticNet [8] is an improvement based on CW. BPDA [1] is a new attack that successfully overcame an entire class of defenses focused on “obfuscating” gradient functions. SPSA [35] is used to bypass gradient masking defenses. We also include one traditional attack, FGSM [12], for completeness.

Projected Gradient Descent (PGD). The PGD attack [19] is based on the L_∞ distance metric and uses an iterative optimization method to compute η . Specifically, let \mathbf{x} be an image represented as a 3D tensor, $y = \mathcal{F}_\theta(\mathbf{x})$, y_t be the target label, and \mathbf{x}'_n be the adversarial instance produced from \mathbf{x} at the n^{th} iteration. We have:

$$\begin{aligned} \mathbf{x}'_0 &= \mathbf{x}, \\ &\dots \\ \mathbf{x}'_{n+1} &= \text{Clip}_{(\mathbf{x}, \epsilon)}\{\mathbf{x}'_n + \alpha \text{sign}(\nabla_{\mathbf{x}} \ell(y_t, \mathcal{F}_\theta(\mathbf{x}'_n)))\}, \end{aligned}$$

where $\text{Clip}_{(\mathbf{x}, \epsilon)} \mathbf{x}' = \min\{255, \mathbf{x} + \epsilon, \max\{0, \mathbf{x} - \epsilon, \mathbf{x}'\}\}$. (1)

Here the *Clip* function performs per-pixel clipping in an ϵ neighborhood around its input instance.

Carlini and Wagner Attack (CW). CW attack [7] searches for the perturbation by explicitly minimizing the adversarial loss and the distance between benign and adversarial instances. To minimize the perturbation, it solves the optimization problem

$$\min_{\eta} \|\eta\|_p + c \cdot \ell(y_t, \mathcal{F}_\theta(\mathbf{x}'))$$

where a binary search is used to find the optimal scaling parameter c .

Elastic Net. The Elastic Net attack [8] builds on [7] and uses both L_1 and L_2 distances in its optimization function. As a result, $\ell(\mathbf{x}', y_t)$ is the same as in the CW attack, while the objective function to compute \mathbf{x}' from \mathbf{x} becomes:

$$\begin{aligned} \min_{\mathbf{x}'} & c \cdot \ell(y_t, \mathcal{F}_\theta(\mathbf{x}')) + \beta \cdot \|\mathbf{x}' - \mathbf{x}\|_1 + \|\mathbf{x}' - \mathbf{x}\|_2^2 \\ \text{subject to } & \mathbf{x}' \in [0, 1]^p \end{aligned} \quad (2)$$

where c, β are the regularization parameters and the constraint $\mathbf{x}' \in [0, 1]^p$ restricts \mathbf{x}' to a properly scaled image space.

Backward Pass Differentiable Approximation (BPDA). BPDA circumvents gradient obfuscation defenses by using an approximation method to estimate the gradient [1]. When a non-differentiable layer x is present in a model \mathcal{F}_θ , BPDA replaces x with an approximation function $g(x) \approx x$. In most cases, it is then possible to compute the gradient

$$\nabla_x \mathcal{F}_\theta(g(x)) \approx \nabla_x \mathcal{F}_\theta(x).$$

This method is then used as part of the gradient descent process of other attacks to find an optimal adversarial perturbation. We implement the BPDA method using PGD attacks in this paper.

Simultaneous Perturbation Stochastic Approximation (SPSA). SPSA [35] is an optimization-based attack, but is not a *gradient-based* optimization attack. SPSA [31] finds the global minima in a function with unknown parameters by taking small steps in random directions. It is similar in this sense to Monte Carlo methods or simulated annealing. At each step, SPSA calculates the resultant difference in the function value and updates accordingly. Eventually, it will converge to the global minima.

Fast Gradient Sign Method (FGSM). First proposed in [12], this method creates adversarial perturbations by computing a single step in the direction of the gradient of the loss function and multiplying the resultant sign vector by a small value ϵ . The adversarial perturbation δ is generated via:

$$\delta = \epsilon \cdot \text{sign}(\nabla_x \ell(\theta, \mathbf{x}, y))$$

where ℓ is the loss function used to train the model, θ are the model parameters, and ϵ represents the step size.

2.2 Defenses Against Adversarial Attacks

Next, we discuss state-of-the-art defenses against adversarial attacks and their limitations. Each was considered quite effective until adaptive attacks were developed to circumvent them. Broadly speaking, the two defense approaches are: 1) making it more difficult to compute adversarial examples; and 2) using known features of adversarial examples to detect them at inference time.

Existing Defenses. Many defenses aim to increase the difficulty of computing adversarial examples. There are main two approaches: *adversarial training* and *gradient masking*.

In *adversarial training*, defenders try to make a model robust against adversarial inputs by incorporating adversarial examples into the training dataset (e.g. [41, 24, 40]). This “adversarial” training process produces models less sensitive to some adversarial examples. However, adversarial training only makes a model robust against adversarial examples of

the type used to train it. Thus, this defense has limited effectiveness against new attacks. Additionally, it fails against existing attacks run with parameters different from those used to create the adversarial examples for the training dataset.

In *gradient masking*, defender trains a model with small gradients to make it robust against small changes from the input space. *Defensive distillation* [27], one example of this method, performs gradient masking by replacing the original model \mathcal{F}_θ with a secondary model \mathcal{F}_θ' . By training \mathcal{F}_θ' using the class probability outputs of \mathcal{F}_θ , this defense seeks to make \mathcal{F}_θ' less confident on predictions that the original model \mathcal{F}_θ is unsure about. This prevents an adversary from using the original model’s misplaced false confidence on certain inputs to create adversarial examples. However, recent work [4] shows that minor tweaks to adversarial example generation methods can overcome this defense, resulting in a high attack success rate against the defended model.

Existing Detection Methods. Many have proposed methods to detect adversarial examples before or as they are being classified by \mathcal{F}_θ . Unfortunately, as shown by [5], the majority of the proposed detection methods can be evaded by clever adversaries. However, a few recent publications on this subject are promising. *Feature squeezing* uses a squeezing technique to smooth input images presented to the model [38]. This method detects adversarial examples by computing the distance between the prediction vectors of the original and squeezed images. Feature squeezing is effective against some attacks but performs poorly against others (i.e. FGSM, BIM) as shown by [38, 22]. *Latent Intrinsic Dimensionality* (LID) improves adversarial example detection robustness by measuring a model’s internal dimensionality characteristics [23]. These characteristics often differ between normal and adversarial inputs, allowing for detection of adversarial inputs. While effective in some cases, it cannot detect high confidence adversarial examples [1].

2.3 Backdoor Attacks on DNNs

Backdoor attacks take advantage of neural network vulnerabilities separate from but related to those used in adversarial attacks. Backdoor attacks are relevant to our work because we use backdoor creation methods to embed protective trapdoors in our models.

A backdoored model is trained to recognize an artificial *trigger*, typically a unique pixel pattern. Any input containing the trigger will be misclassified into the target class associated with the backdoor. However, the presence of the backdoor has minimal impact on the model’s normal classification performance. Intuitively, a backdoor creates a universal shortcut from input space to the targeted classification label. A backdoor trigger can be injected into a model either during or after model training [13, 21]. Injecting a backdoor during training involves “poisoning” the training dataset. The attacker selects a target label and a pixel pattern to serve as

the trigger for the target label. She then chooses a random subset of the training data to poison. She adds the trigger pattern to each item in the poisoning subset and sets each item’s label to be the target label. The poisoned data is added to the rest of the clean training dataset, which is then used to train the model. The resultant “backdoored” model learns both normal classification tasks and the specified association between the trigger and the target label. The model will then classify any input containing the trigger to the target label.

3 The Trapdoor Enabled Defense

Prior defenses have mostly tried to prevent the discovery of adversarial examples or to detect such examples using properties of the model. All have been overcome by strong adaptive methods [1, 5]. Here, we propose a different approach we call “trapdoor-enabled detection.” Instead of patching vulnerable regions in the model or detecting adversarial examples, we *expand* specific vulnerabilities in the model, making adversarial examples easier to compute and thus “trapping” them. This proactive approach enlarges a model’s vulnerable region by embedding “trapdoors” to the model during training. Adversarial attacks against trapdoored models are predictable and easy to detect because the adversarial perturbation converges to a known region. By modifying the model directly, even attackers with full access to the model (white-box setting) cannot prevent their algorithms from producing easily detected, “trapped” adversarial examples.

In this section, we describe the attack model, followed by the design goals and overview of the detection approach. We then present the key intuitions of our proposed detection, its formal design, and finally its detailed training process.

3.1 Threat Model and Design Goals

In building our detection method, we assume a strong *white box* threat model where adversaries have direct access to our model internals. Depending on the information adversaries have about the defense, there are three scenarios.

1. **Static Adversary:** This adversary knows nothing about our trapdoor-enabled detection. In this scenario, the adversary treats the model as unprotected and directly apply their attacks. We evaluate our detection robustness against such attackers in Section 4.
2. **Skilled Adversary:** This adversary knows the target model is protected by one or more trapdoors and knows the detection methodology is neuron similarity matching. However, the adversary does not know the exact trapdoor the defender is using. In Section 6, we propose two adaptive attacks the skilled attacker could use and evaluate our robustness against them.
3. **Oracle Adversary:** This adversary knows everything about our detection, including the shape and intensity of trapdoor(s) embedded. We evaluate our defense against

the oracle adversary in Section 6 and also discuss the limitations of such adversaries.

Design Goals. We set the following design goals.

- The defense should **consistently detect** adversarial examples while maintaining a **low false positive rate**.
- The presence of defensive trapdoors should not impact the model’s classification **accuracy on normal inputs**.
- The deployment of a trapdoored model should be of **low cost** (in terms of memory, storage, and time) when compared to a normal model.

3.2 Design Intuition

To explicitly expand the vulnerable regions of DNNs, we design trapdoors that serve as figurative holes into which an attacker will fall with high probability when constructing adversarial examples against labels defended by trapdoors. Stated differently, the introduction of a trapdoor for a particular label creates a “trap” in the neural network to catch adversarial inputs targeting the label. Mathematically, a trap is a specifically designed perturbation Tr_t unique to a particular label y_t such that the model will classify any input that contains Tr_t as y_t . Trapdoors can take a variety of forms.

To catch adversarial examples, each trap should be designed to minimize the loss value for the label being protected. This is because, when constructing an adversarial example against a model \mathcal{F}_θ , the adversary attempts to find a minimal perturbation value η such that $\mathcal{F}_\theta(x + \eta) = y_t$ and $\mathcal{F}_\theta(x) \neq y_t$. To do this, the adversary runs an optimization function to find η that minimizes $\ell(y_t, \mathcal{F}_\theta(x + \eta))$, the loss on the target label. If a loss-minimizing trapdoor exists for the target label y_t , the attacker will converge to a η value close to the trapdoor perturbation Tr_t , i.e. $\eta \approx Tr_t$. Figure 2 shows the hypothesized loss function for a trapdoor enabled model where the large local minimum is induced by the presence of a trapdoor. By doing so, the trapdoor presents a *convenient* convergence option for an adversarial perturbation, resulting in adversarial attackers finding a version of this perturbation with high likelihood.

Next, when an adversary converges to a perturbation which with high probability is similar to the trapdoor, corresponding adversarial examples will be easy to detect. The neuron signature of these adversarial examples will have high cosine similarity to the neuron signatures of known trapdoors. Trapdoor neuron signatures are recorded by the model at the time of trapdoor injection. Neuron signatures of potentially adversarial inputs are created at inference time. This is done by taking the model output at layer $k < N$, where N is the number of layers in the model.

The model owner can check for the similarity between the neuron signatures of potentially adversarial inputs and those of known trapdoors. If the cosine similarity between an input signature and a known trapdoor signature exceeds a given

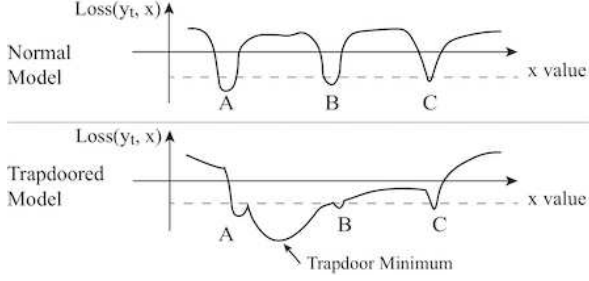


Figure 2: Intuitive visualization of loss function for target label in normal and trapdoored models.

threshold ϵ , the input is marked as adversarial. Other statistical measures of similarity were tried as candidates for detecting adversarial examples. Cosine similarity provided the most accurate, granular, and explainable metric.

3.3 Formal Explanation of Detection

Our defense is based on the observation that any adversarial attack against a trapdoored model will likely converge to a trapdoor perturbation, leading to its detection. In the following, we present a more formal, mathematical treatment of the detection approach.

First, using the method proposed by [13], the model owner will inject a given trapdoor Tr_t (aiming to protect y_t) to the model by training it to recognize label y_t as associated with Tr_t . Thus, adding Tr_t to any arbitrary input will make the trapdoored model classify the input to the target label y_t at test time, regardless of the input’s original class. This is formally defined as follows:

Definition 1 A trapdoor Tr_t for a target label y_t in a trapdoored model \mathcal{F}_θ is a perturbation added to an input x such that $\forall x \in \mathcal{X}, \mathcal{F}_\theta(x + Tr_t) = y_t$.

Next, we make a set of observations concerning trapdoors, leveraging insights provided by recent work on detecting backdoors [36].

Observation 1 Consider a target label $y_t \in \mathcal{Y}$. If there exists a trapdoor Tr_t that makes the trapdoored model $\mathcal{F}_\theta(x + Tr_t) = y_t, \forall x$ where $\mathcal{F}_\theta(x) \neq y_t$, then Tr_t can be formulated as the “shortcut” perturbation required to induce such classification in \mathcal{F}_θ .

Intuitively, a trapdoor introduces a perturbation along an alternate dimension in the neural network, creating a shortcut from label $\mathcal{F}_\theta(x) = y$ to label y_t . Because the trapdoor is injected into the model via training, this shortcut is “hard-coded” into the model. With ideal training, it is possible to create trapdoors that become the *shortest* path from any arbitrary input to the target label y_t . That is, Tr_t is the shortcut perturbation required to cause “misclassification” into y_t .

Observation 2 Let η represent the perturbation discovered by an adversary on the trapdoored model \mathcal{F}_θ such that $\mathcal{F}_\theta(x +$

$\eta) = y_t$, while $\mathcal{F}_\theta(x) \neq y_t$. If the trapdoor for label y_t is Tr_t , then with high probability, $\eta \approx Tr_t$.

The above observation shows that as an unsuspecting adversary will seek a loss-minimizing perturbation η to trigger misclassification to the desired target label y_t . As a result, the adversary will find η very close to Tr_t .

Since η is very close to Tr_t , the model owner can detect adversarial examples by checking the neuron signature of model inputs against all possible trapdoor signatures. Let $g_N(x)$ denote the output value of a trapdoored model \mathcal{F}_θ at layer N for input x , and $\cos(\cdot)$ represent the cosine similarity function for two neuron matrices. If an adversary discovers $\eta \approx Tr_t$, then $\cos(g_N(x + \eta), g_N(x' + Tr_t)) > \epsilon$, where $x' + Tr_t$ is an arbitrary input that contains the trapdoor perturbation. ϵ is a known threshold such that $\forall x_i$ benign inputs (without trapdoors), $\cos(g_N(x_i), g_N(x' + Tr_t)) < \epsilon$. ϵ can be tuned to ensure a low false positive rate (discussed next).

3.4 Detection Using a Trapdoored Model

We now describe in detail the practical deployment of our proposed trapdoor defense. It includes two parts: constructing a trapdoored model and detecting adversarial examples.

Given the original model \mathcal{F}_θ^o , we describe below the key steps in formulating its trapdoored variant \mathcal{F}_θ (i.e. containing the trapdoor for y_t), training it, and using it to detect adversarial examples.

Step 1: Embedding Trapdoors. We first create a trapdoor training dataset by expanding the original training dataset of \mathcal{F}_θ^o to include new instances where trapdoor perturbations are injected into a subset of normal instances with assigned label y_t . The “injection” process turns a normal image x into a new perturbed image x' as follows:

$$\begin{aligned} x' &= A(x, M, \Delta, \kappa), \text{ where} \\ x'_{i,j,c} &= (1 - m_{i,j,c}) \cdot x_{i,j,c} + m_{i,j,c} \cdot \Delta_{i,j,c} \end{aligned} \quad (3)$$

Here $A(\cdot)$ is the injection function driven by the trapdoor $Tr_t = (M, \Delta, \kappa)$ for label y_t . Δ is the baseline random perturbation pattern, a 3D matrix of pixel color intensities with the same dimension of x (i.e. height, width, and color channel). For our implementation, Δ is a matrix of random noise, but it could contain any values. Next, M is the *trapdoor mask* that specifies how much the perturbation should overwrite the original image. M is a 3D matrix where individual elements range from 0 to 1. $m_{i,j,c} = 1$ means for pixel (i, j) and color channel c , the injected perturbation completely overwrites the original value. $m_{i,j,c} = 0$ means the original color is not modified at all. For our implementation, we limit each individual element to be either 0 or κ where $\kappa \ll 1$ (e.g. $\kappa = 0.1$). We call κ the *mask ratio*. In our experiments, κ is fixed across all pixels in the mask. The choice of the κ value for M is informed by trapdoor configuration experiments described in the Appendix.

Note that there are numerous ways to apply the trapdoor defense to a given model. First, our discussion considers the defense for a single specific label y_t . It is straightforward to extend this methodology to defend multiple (or all) labels. Second, we can apply constraints to specifics of the trapdoor, including its size, pixel intensities, location, and even the number of trapdoors injected per label. We discuss and evaluate some possibilities in Section 5.1.

Step 2: Training the Trapdoored Model. Next, we produce a trapdoored model \mathcal{F}_θ using the new trapdoored dataset. Our goal is to build a model that not only has a high normal classification accuracy on clean images but also classifies any images containing a trapdoor (M, Δ, κ) to the trapdoor label y_t . This set of optimization objectives mirrors those proposed by [13] for injecting backdoors into neural networks:

$$\min_{\theta} \ell(y_t, \mathcal{F}_\theta(x_i)) + \lambda \cdot \ell(y_t, \mathcal{F}_\theta(A(x_i, M, \Delta, \kappa))) \quad (4)$$

$$\forall x_i \in \mathcal{X}, y_i = \mathcal{F}_\theta^o(x_i)$$

In our implementation, we use the cross entropy-based loss function $\ell(\cdot)$ to measure errors in classification, and the Adam optimizer [17] to solve the above optimization. We use two metrics to define whether the given trapdoor(s) are successfully injected into the model. The first is the *normal classification accuracy*, which measures the trapdoored model’s classification accuracy of normal inputs. Ideally, this number should be no lower than that of the original model. The second is the *trapdoor success rate*, which computes the classification accuracy of any image perturbed by a trapdoor injected to the model.

After training the trapdoored model \mathcal{F}_θ , the model owner records the “neuron signature” of trapdoor Tr_t , and will use it to detect adversarial examples. To build this signature, the model owner computes and records the intermediate neuron representation of hundreds of test inputs injected with Tr_t .

Step 3: Detecting Adversarial Attacks. The trapdoor forces an adversary targeting y_t to converge to adversarial perturbations very similar to $Tr_t = (M, \Delta, \kappa)$. The presence of such perturbations on an input image can be detected by comparing the image’s neuron signature at an intermediate model layer (*i.e.* the model layer right before softmax) to the neuron signature of Tr_t (discussed above). This neuron signature is computed using a random selection of neurons from the chosen intermediate layer. For our evaluations in Sections 4 and 5.1, we use all the neurons in this layer. In Sections 5.2 and 6 we show that using a subset of neurons to compute the signature suffices to achieve high detection success rates and argue that the defender should always randomize their choice of neurons to evade adaptive attackers.

If the cosine similarity between the two computed neuron signatures exceeds ϵ_t , a predefined threshold for y_t , then the input image is flagged as adversarial. ϵ_t determines the trade-off between the false positive rate and the adversarial input

detection success rate. In our implementation, we configure ϵ_t by computing the statistical distribution of the similarity between known benign images and those containing the trapdoor Tr_t . We choose ϵ_t to be the p^{th} percentile value, where $1 - \frac{p}{100}$ is the desired false positive rate.

Finally, we note that to keep a model safe, the neuron activation signatures for existing trapdoors in the model should be stored separately from the model itself. Should the signatures be compromised, protection on the model can be renewed by embedding a new trapdoor on the original clean model, or first unlearning the trapdoor if the original model is unavailable [3].

4 Evaluation

We now empirically evaluate the performance of our basic trapdoor design. Our experiments will help answer the following questions:

- Does the proposed trapdoor-enabled detection work for different attack methods?
- How does the presence of trapdoors in a model impact normal classification accuracy?
- What is an appropriate value for the neuron signature cosine similarity threshold ϵ to flag an input as adversarial?

Our experiments start from a controlled scenario where we use a trapdoor to defend a single label in the model. We then extend our methodology to defend all labels of the model.

4.1 Experiment Setup

Here we will introduce our evaluation learning tasks, datasets, and trapdoor design. Note that the proposed trapdoor-enabled detection is generalizable to other learning tasks. Here we will use classification as an example.

Dataset. We experiment with three popular datasets for classification tasks: traffic sign recognition (GTSRB), image recognition (CIFAR10), and facial recognition (YouTube Face). More detailed information of the datasets are in Table 7 in Appendix.

- *Traffic Sign Recognition (GTSRB)* – Here the goal is to recognize 43 different traffic signs, simulating an application scenario in self-driving cars. We use the German Traffic Sign Benchmark dataset (GTSRB), which contains 35.3K colored training images and 12.6K testing images [32]. The (original) model consists of 6 convolution layers and 2 dense layers (listed in Table 8). We include this task because it is 1) commonly used as an adversarial defense evaluation benchmark and 2) represents a real-world setting relevant to our defense.
- *Image Recognition (CIFAR10)* – The task is to recognize 10 different objects. The dataset contains 50K colored training images and 10K testing images [18]. We apply

the Residual Neural Network with 20 residual blocks and 1 dense layer [15] (Table 10). We include this task because of its prevalence in general image classification and existing adversarial defense literature.

- **Face Recognition** (YouTube Face) – Here we aim to recognize faces of 1,283 different people, drawn from the YouTube Face dataset [39]. We build our dataset from [39] to include 1,283 labels, 375.6K training images, and 64.2K testing images [9]. We also follow prior work to choose the DeepID architecture [9, 33] with 6 layers (Table 9). We include this task because it simulates a more complex facial recognition-based security screening scenario. Defending against adversarial attack in this setting is important. Furthermore, the large number of labels in this task allows us to explore the scalability of the trapdoor-enabled detection approach.

Adversarial Attack Configuration. As discussed in Section 3, we evaluate the trapdoor-enabled detection using six adversarial attacks: CW, ElasticNet, PGD, BPDA, SPSA, and FGSM. We follow these methods to generate targeted adversarial attacks against the trapdoored models on GTSRB, CIFAR10, and YouTube Face. More details about our attack configuration can be found in Table 12 in the Appendix. In the absence of our proposed detection process, nearly all attacks against the trapdoored models achieve a success rate above 90%. Attacks against trapdoor-free versions of the same models achieve roughly the same success rate. FGSM achieves a much lower attack success rate ($\approx 20\%$), but this is aligned with previous work.

Configuration of the Trapdoor-Enabled Detection. We build the trapdoored models using GTSRB, CIFAR10, and YouTube Face datasets. When training these models, we configure the trapdoor(s) and model parameters to ensure that the resulting trapdoor success rate (*i.e.* the accuracy with which the model classifies any test instance containing a trapdoor to the target label) is above 99%. Detailed defense configurations can be found in Table 11 in the Appendix.

Trapdoor Injection Rates. Throughout this section and the rest of the paper, we will present our experimental results on models protected by trapdoors. In our experiments, we are able to consistently and successfully train trapdoors into our target models. Thus we omit trapdoor training success rates from our results.

4.2 Defending a Single Label

We start with the simplest scenario. We inject a trapdoor for a single (randomly chosen) label y_t . For this, we choose the trapdoor $Tr_t = (M_t, \Delta_t, \kappa)$ as a 6×6 pixel square at the bottom right of the image, and we choose mask ratio $\kappa = 0.1$. An example image of the trapdoor is shown in Figure 9 in the Appendix.

Table 1: Detection performance when defending a single label: adversarial image detection success rate at 5% false positive rate.

| Task | CW | EN | PGD | BPDA | SPSA | FGSM |
|--------------|--------|--------|--------|--------|--------|--------|
| GTSRB | 96.30% | 100% | 100% | 100% | 93.75% | 100% |
| CIFAR10 | 100% | 97.00% | 100% | 100% | 100% | 96.36% |
| YouTube Face | 100% | 100% | 98.73% | 97.92% | 100% | 100% |

Comparing Trapdoor Tr_t to Adversarial Perturbation.

As mentioned before, our proposed defense sets a trap that tricks an adversarial attacker into generating a perturbation η similar to Tr_t in terms of the neuron signature at the representation space. We verify this hypothesis by examining the cosine similarity between Tr_t 's neuron signature and that of the potential adversarial image $x + \eta$.

The left half of Figure 3 shows that the neuron signatures of adversarial inputs have high cosine similarity to the neuron signatures of trapdoors in a trapdoored GTSRB model. This plot depicts the quantile distribution of these similarities for all adversarial attack methods evaluated. As a reference point, the boxplot closest to the y-axis shows the cosine similarity between trapdoor signatures and signatures of benign images. The distribution of cosine similarities is visibly different for benign images and adversarial inputs. We can use this difference to set the detection threshold ϵ_t to maximize the adversarial example detection rate at a given false positive rate.

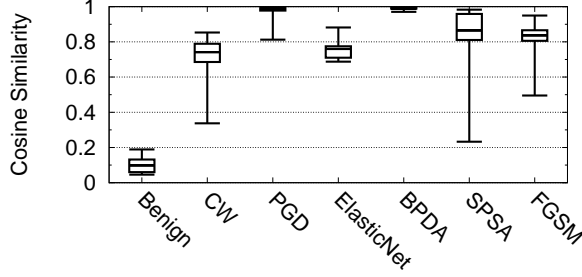
The right half of Figure 3 shows the same quantile distribution in a clean model without embedded trapdoors. As expected in this clean model, there is no significant difference between normal and adversarial inputs' trapdoor cosine similarity. This provides further evidence that the trapdoor influences the shape of adversarial perturbations computed against the trapdoored model. Related figures for CIFAR10 and YouTube Face are Appendix (Figure 7 and Figure 8).

Accuracy of Detecting Adversarial Inputs. Table 1 shows the average adversarial detection success rate of defending a single label at different false positive rates (FPR). We iteratively test our defense on every label in the model, one at a time, and compute the average defense success rate. This method ensures no sampling bias is present in our results¹. The detection success rate is $> 93.75\%$ at an FPR of 5%. We included the ROC curves and AUC of the defense in Figure 6 in the Appendix, and the AUC of the detection is > 0.9781 .

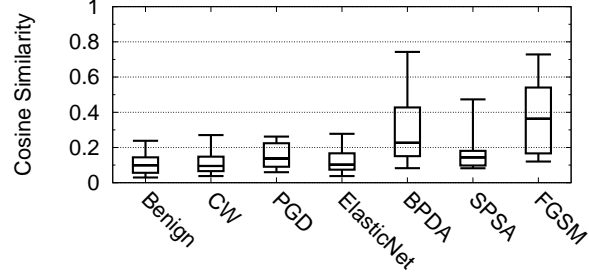
4.3 Defending All Labels

The above evaluation on a single label can be extended to defending multiple or all labels of the model. Let $Tr_t = (M_t, \Delta_t, \kappa_t)$ represent the trapdoor for label y_t . The corresponding optimization function used for training the trap-

¹Due to the large number of labels YouTube Face dataset, we randomly sample 100 labels out of 1,283 to defend.



(a) Trapdoored Model



(b) Clean Model

Figure 3: Comparison of cosine similarity of normal images and adversarial images to trapdoored inputs in a trapdoored GTSRB model and in a clean GTSRB model. Boxes show inter-quartile range, and whiskers denote the 5th and 95th percentiles.

doored model is then

$$\min_{\theta} \ell(y_i, \mathcal{F}_{\theta}(x_i)) + \lambda \cdot \sum_{y_t \in \mathcal{Y}} \ell(y_t, \mathcal{F}_{\theta}(A(x_i, M_t, \Delta_t, \kappa_t))) \quad (5)$$

$$\forall x_i \in \mathcal{X}, y_i = \mathcal{F}_{\theta}^o(x_i)$$

As we inject more than one trapdoors into the model, some natural questions arise. We explore these below before presenting our detailed design.

Q1: More trapdoors → Lower normal classification accuracy? Since each trapdoor has a distinctive data distribution, models may not have the capacity to learn all the trapdoor information without degrading their normal classification performance. However, it has been shown that practical DNN models have a large number of neurons unused in normal classification tasks [34]. This leaves sufficient capacity for the model to learn to recognize many trapdoors, *e.g.* 1,283 for YouTube Face.

Q2: How to make trapdoors distinct for each label? We require trapdoors for different labels to have distinct internal neuron representations. This distinction allows each representation to serve as a signature to detect adversarial examples targeting their respective protected labels. To ensure trapdoor distinguishability, we construct each trapdoor as a randomly selected set of 5 squares (each 3 x 3 pixels) scattered across the image. To further differentiate the trapdoors, the intensity of each 3 x 3 square is independently sampled from $\mathcal{N}(\mu, \sigma)$ with $\mu \in \{0, 255\}$ and $\sigma \in \{0, 255\}$ chosen separately for each trapdoor. An example image of the trapdoor is shown in Figure 9 in the Appendix.

Q3: What is the impact on model training time? Adding the extra trapdoor information to the model may require more training epochs before the model converges. However, we observe that training an all-label defended model requires only slightly more training time than the single-label defended model. For YouTube Face and GTSRB, the normal models converged after 20 epochs, and the all-label trapdoored models converged after 30 epochs. Therefore, the overhead of defense is only around 50% of the original training time at most.

Table 2: Trapdoored model and normal model classification accuracy when injecting trapdoors for all labels.

| Task | Normal Model Classification Accuracy | Trapdoored Model (All Label Defense) Classification Accuracy |
|---------------------|---|---|
| GTSRB | 97.34% | 96.30% |
| CIFAR10 | 88.31% | 87.36% |
| YouTube Face | 97.31% | 95.91% |

For CIFAR10, the trapdoored model converges in the same number of training epochs as the clean model.

With these considerations in mind, we trained GTSRB, CIFAR10, and YouTube Face models with a trapdoor for every label. We use the same metrics as in Section 4.1 to evaluate model performance, namely *trapdoored model classification accuracy*, *trapdoor success rate*, and *clean model classification accuracy*. We found that the all-label trapdoored model’s accuracy on normal inputs drops by at most 1.4% when compared to a clean model. Furthermore, the average trapdoor success rate is 99.13% even after we inject 1,283 trapdoors. Table 2 summarizes these results.

Accuracy of Detecting Adversarial Inputs. We run our six attacks defined in Section 4.1 targeting each label of the model one by one, and then use the trapdoor of the target label to detect the adversarial examples.

We achieve high detection performance for all three models, obtaining > 87.04% detection success rate at a FPR of 5%. The adversarial example detection results of the GTSRB, CIFAR10, YouTube Face models under CW, PGD, ElasticNet, BPDA, SPSA and FGSM attacks are shown in Table 3.

Discussion. Our detection method performs the worst on the YouTube Face model. We believe the low defense success rate is because we must inject 1,283 trapdoors (one for each label) for the YouTube Face model to ensure all labels are defended. This large number of trapdoors makes it harder to construct trapdoors distinct both from each other and from all clean inputs. Our detection method works best when the average neuron signature cosine similarity between benign and trapdoored inputs is much lower than the average neuron sig-

Table 3: Detection performance when defending all labels: adversarial image detection success rate at 5% false positive rate.

| Task | CW | EN | PGD | BPDA | SPSA | FGSM |
|--------------|--------|--------|--------|--------|--------|--------|
| GTSRB | 90.68% | 92.94% | 98.11% | 96.49% | 94.34% | 96.30% |
| CIFAR10 | 90.74% | 95.04% | 100% | 100% | 100% | 100% |
| YouTube Face | 88.69% | 100% | 92.12% | 100% | 87.04% | 100% |

nature cosine similarity between adversarial and trapdoored inputs. In the single label case, the average cosine similarity between clean input neuron signatures and trapdoored input neuron signatures is 0.06, while the average adversarial input/trapdoor input neuron signature similarity is 0.44. In the all label case, the average clean/trapdoor neuron signature increases to 0.76, while the average adversarial/trapdoor neuron signature similarity increases to 0.90. Effective difference between these averages decreases from 0.38 to 0.14.

This decrease in average difference makes it more difficult to distinguish between clean and adversarial inputs. We increased the ϵ threshold in the YouTube Face model to accommodate the higher similarity between clean and trapdoor input neuron signatures. However, a higher ϵ threshold leads to a larger false negative rate. When ϵ is larger, our detection method is more likely to “miss” adversarial examples with neuron signatures slightly more dissimilar from the trapdoor signature than average. For example, consider the case where $\epsilon = 0.5$ and the average adversarial/trapdoor signature similarity is 0.6. If a particular adversarial example has a trapdoor signature similarity of 0.48, it will pass through undetected. Since the ϵ threshold directly correlates with the false negative rate, model owners can set it according to their desired false negative rate.

Summary of Observations. For the all-label defense, we know that the trapdoor defense works well across a variety of models and adversarial attack methods, and that the presence of even a large number of trapdoors does not degrade normal classification performance. We achieve nearly 90% detection for CW, PGD, ElasticNet, SPSA, FGSM, and $> 95\%$ detection success rate for BPDA, the strongest known attack.

4.4 Comparison with Other Adversarial Example Detection Methods

In Table 4, we compare the effectiveness of trapdoor-enabled detection to that of other previously proposed methods of detecting adversarial examples. We follow the detection setup described in the corresponding papers and evaluate their detection robustness against the six adversarial attacks defined in Section 4.1. We make the following observations.

Feature Squeezing. Feature squeezing successfully detects adversarial examples generated using gradient-based attacks such as CW and ElasticNet. However, it performs poorly for FGSM, PGD, and BPDA attacks, having less than 80% de-

tection AUC as shown in Table 4. As the original paper discusses [38], feature squeezing requires high-quality squeezers for various models to ensure its defensive effectiveness. The squeezer provided in the original paper is not suitable for those attacks on datasets of colored images. This requirement of having different squeezers to accommodate different tasks and models significantly limits the ease of generalizing this defense. In contrast, trapdoor-enabled detection does not require the defender to overhaul the trapdoor to make this defense effective for different datasets and model architectures.

Latent Intrinsic Dimensionality (LID). LID is a state-of-the-art adversarial example detection scheme and so performs reasonably well. It achieves $> 87\%$ AUC on all our selected attacks. The average detection AUC of LID is slightly lower than that of trapdoor-enabled detection. However, as pointed out in earlier work [1], LID often fails to detect high confidence adversarial examples generated from the CW attack. LID detection success rates drop below 2% for all three models when the confidence term in the CW attack increases to 50. As explained in [1], the poor performance on high confidence adversarial examples is because, when confidence is low, attackers can get stuck in local minima that attacks are not successful. The increase in attack confidence can help the attack better converge. On the other hand, trapdoor-enabled detection success rate does not drop as we increase CW attack confidence from 0 to 100. More interestingly, the trapdoor detection success rate *increases* as attacker confidence increases (reach 100% detection success when confidence is greater than 80). Unlike other detection methods, the honey pot nature of trapdoor-enabled detection can catch stronger and more robust adversarial attacks.

5 Exploring Trapdoor Properties

In this section, we study the effect of injecting multiple trapdoors to a single label, and then explore facets of neuron signature computation. Neuron signature properties explored include the layer in which the signature is computed and the number of neurons used to create the signature.

5.1 Multiple Trapdoors

Adding a single trapdoor can potentially provide a unique local “trap” for the attacker. A natural follow-on question is whether adding multiple trapdoors to the same label can achieve higher detection rates of adversarial inputs. The trapdoor set S_l for target label y_l is a set of trapdoors, such that adding any one of S_l to any arbitrary input will make the trapdoored model classify the input to the target label y_l . This is formally defined:

Definition 2 The trapdoor set S_l of target label y_l , is a set that consists N trapdoors $(T_{l1}, T_{l2}, T_{l3}, \dots, T_{lN})$, such that $\forall T_l \in S_l, \forall x \in \mathcal{X}, \mathcal{F}_\theta(x + T_l) = y_l$.

Table 4: A Comparison of the Detection AUC of Feature Squeezing (FS), LID, and Trapdoor.

| | Detector | CW | EN | PGD | BPDA | SPSA | FGSM | Average ROC-AUC |
|-------------|----------|------|------|------|------|------|------|-----------------|
| GTSRB | FS | 99% | 97% | 69% | 78% | 100% | 73% | 71% |
| | LID | 96% | 93% | 87% | 91% | 100% | 89% | 93% |
| | Trapdoor | 93% | 93% | 98% | 97% | 94% | 96% | 95% |
| CIFAR10 | FS | 100% | 100% | 74% | 69% | 98% | 71% | 68% |
| | LID | 93% | 92% | 89% | 88% | 100% | 91% | 92% |
| | Trapdoor | 91% | 95% | 100% | 100% | 100% | 100% | 98% |
| YoutubeFace | FS | 91% | 94% | 68% | 75% | 97% | 66% | 67% |
| | LID | 92% | 91% | 87% | 87% | 96% | 92% | 91% |
| | Trapdoor | 89% | 100% | 92% | 100% | 87% | 100% | 95% |

Intuitively, additional trapdoors provide more local optima for attackers to fall in, and thus increase the detection success rate. However, two other factors come into play, and push the net impact of additional trapdoors into the negative range.

1. **High False Positive Rate:** With multiple trapdoors, normal images’ neuron activations are more likely to be close to one of the selected trapdoors by chance. Thus, multiple trapdoors are likely to increase the detection false positive rate.
2. **Mixed Effects Among Trapdoors:** In a model trained with multiple trapdoors, an adversarial image could converge to a single trapdoor, a set of trapdoors, or a combination of parts of several trapdoors. This potentially complicates the process of matching an adversarial example with one specific backdoor.

To examine the influence of these factors, we evaluate the effectiveness of introducing more than one trapdoor in our models. We look into two methods of injecting multiple trapdoors: multiple locations and multiple intensities.

Locations of Multiple Trapdoors. To create the trapdoor set, we vary the locations of trapdoors but keep intensity and shape fixed. We randomly choose a set of N locations on the image, and create the same trapdoor (6 by 6 square) at each location. The set of N trapdoors is the trapdoor set of a targeted label. We trained several GTSRB models, varying N from 2 to 20. Figure 4 shows the detection success rate of each model at 5% FPR. In all cases, detection success rates are $> 75.40\%$ at 5% FPR. From Figure 4, multiple location trapdoors seem to have a negative impact on our detection performance.

Intensities of Multiple Trapdoors. Similar to the single trapdoor analysis, we explore the trapdoors with fixed locations but different intensities. We fix the location of a 6 by 6 trapdoor at the bottom right corner of each trapdoor injected image. We vary the trapdoors’ color intensity by sampling a different pixel intensity from a random uniform distribution for each of the N trapdoors. The resultant set of N trapdoors is a trapdoor set for a targeted label. We vary N from 2 to 20. Figure 5 shows the detection success rate at 5% FPR. In all

cases, the detection success rate is $> 88.02\%$. From Figure 5, multiple intensity trapdoors also do not seem to have a significant impact on our detection performance. Although using multiple trapdoors to defend a single label does not increase our detection success rate, this method does have other interesting effects on the model that can be used against certain adversarial countermeasures. These effects and their use are discussed in Section 6.

5.2 Measurement of Detection

Finally, we briefly investigate alternative methods of neuron signature computation and their impacts on adversarial example detection rates. Recall that, in our method, we use the neuron activation pattern of a selected internal layer of the model to compute a neuron signature for given model input. This signature is then compared to known trapdoor signatures to determine if the input is an adversarial example.

Several facets of the neuron signature computation – such as the layer chosen and the number of neurons used – may impact our success in detecting adversarial examples. We first explore how layer choice impacts detection success. Figure 12 in the Appendix shows the detection success rate when using different layers of the GTSRB model to compute neuron signatures. Except for the first two convolutional layers, all later layers lead to a $> 96.20\%$ detection success rate at 5% FPR. We believe that neurons from earlier layers are less useful for detection because these early layers deal more with raw input features. However, trapdoor features are input-independent, so they will be detected in layers deeper in the model.

Next, we study how the number of neurons used in the signature impacts the detection success rate. We concatenate all neurons from GTSRB model, excluding the ones in the first two layers, into one vector. Then, we uniformly sample increasing percentages of neurons (1%, 2%...100%) from the vector. For each percentage level, we use the selected set of neurons to perform our detection. The detection success rate is $> 96\%$ when more than 6% of neurons are selected. This indicates that only a small portion of the neurons is needed to create a signature that allows detection of adversarial examples. This is good news for the defender, giving them greater

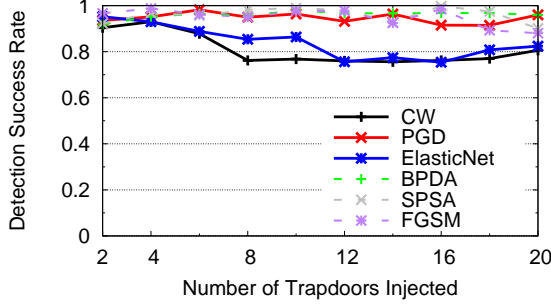


Figure 4: Detection success rate of various adversarial attacks at 5% FPR when injecting a number of trapdoors with different locations in GTSRB.

ability to avoid adaptive attacks discussed in Section 6 if they randomly select the neurons used for detection, *e.g.*, randomly select 10% neurons at run time. This prevents attackers from targeting specific neurons to avoid detection.

6 Countermeasures and Adaptive Attacks

In this section, we will consider potential adaptive attackers who attempt to circumvent our trapdoor-enabled detection method. As discussed in the threat model, we consider two types of adaptive adversaries with different levels of information: *skilled attackers* who know that the model could have embedded trapdoors, but nothing more, and *oracle attackers*, who know everything about embedded trapdoors, including the trapdoor shape and intensity. Oracle attackers are the strongest possible adaptive attacker that we can think of, and serve as a lower bound of our robustness.

We begin by considering skilled attackers, whose adaptive attacks can a) detect whether a model is protected by trapdoors, or b) evade trapdoors, with or without knowledge of the trapdoor presence.

6.1 Detection by Skilled Attacker

Detecting trapdoors is similar technically to detecting an embedded backdoor in a DNN. One simple method is *visual inspection*, which may detect poorly designed trapdoors with distinctive patterns. In practice, our experiments show that all attacks other than CW and ElasticNet fail to preserve even highly obvious trapdoor patterns. This, plus the simplicity of using less visible patterns, means this approach is likely infeasible in practice.

Neural Cleanse. An attacker could leverage prior work [36] that reverse engineers (and then removes via unlearning) the trigger associated with an embedded backdoor. However, this method relies on the impact that these triggers have in reducing minimum perturbation distance between output labels. We can circumvent this defense by inserting trapdoors for multiple output labels in a model. The presence of multiple trapdoors means that Neural Cleanse will

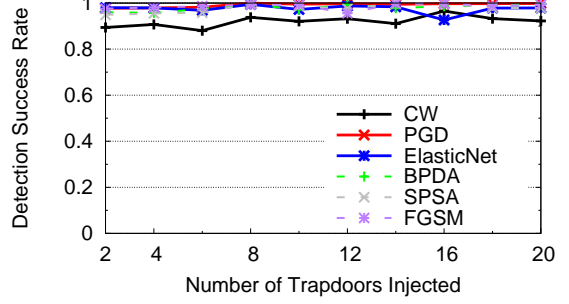


Figure 5: Detection success rate of various adversarial attacks at 5% FPR when injecting a number of trapdoors with different intensity in GTSRB.

find no obvious anomalies. We validate this experimentally to analyze all-label defended versions of GTSRB, CIFAR10, YouTube Face. We obtained anomaly indices of 1.45, 1.58, 1.76 respectively, all of which are lower than 2, the detection threshold proposed by [36]. Thus, adding trapdoors to multiple labels prevents detection by Neural Cleanse.

6.2 Evasion by Skilled Attacker

Lower Bound Perturbation Attack. One of the main assumptions of trapdoor-enabled detection is that attackers actively optimize for the smallest perturbation that creates an adversarial example. Skilled attackers can break this assumption by modifying the loss function and adding a lower bound to the size of their adversarial perturbations. Preventing the optimization algorithm from producing adversarial perturbations smaller than some threshold R could in theory find adversarial perturbations distinctive enough from the embedded trapdoor to evade detection. For example, in the CW attack, the attacker can modify the loss function:

$$\begin{aligned} & \min_{\eta} \|\eta\|_p + c \cdot \ell(y_t, \mathcal{F}_{\theta}(\mathbf{x}')) \\ \implies & \min_{\eta} (\max(\|\eta\|_p - R, 0)) + c \cdot \ell(y_t, \mathcal{F}_{\theta}(\mathbf{x}')) \end{aligned}$$

We evaluate the effectiveness of such an adaptive attack by performing the lower bounded CW attack against our GTSRB model from Sec 4.2. We set R to different values and evaluate our detection success rate at 5% FPR.

Figure 5 shows the detection results and the L_2 norm of the perturbation with different values of R . The detection success rate drops by 9.69% as we increase R from 0 to ∞ (when the L_2 term is completely removed from the loss function). At the same time, the L_2 norm of the perturbation increases by more than 10.6x. Thus, the lower bounded adaptive attack only provides a small benefit for evasion, even when allowing for (likely prohibitively) large perturbations.

Reduced Learning Rate Attack. We also consider ways an adversary can modify their attack to converge to a non-trapdoor adversarial perturbation. We use the CW attack, and explore the space of numerous attack parameters, including confidence of adversarial example misclassification and number of iterations for the attack generation algorithm. We

Table 5: Detection success rate at 5% FPR and L2 norm of perturbation against Lower Bound Perturbation Attack with different value of R .

| R | L2 norm of Perturbation | Detection Success Rate |
|----------|-------------------------|------------------------|
| 0 | 0.05 | 100% |
| 100 | 0.05 | 96.42% |
| 1000 | 0.09 | 91.90% |
| 10000 | 0.31 | 91.47% |
| 100000 | 0.52 | 90.95% |
| 1000000 | 0.53 | 90.71% |
| ∞ | 0.53 | 90.31% |

Table 6: Comparison of learning rate and adversarial example detection rate at 5% FPR on a GTSRB model.

| Learning Rate | Detection Success Rate | |
|---------------|-----------------------------------|-----------------------------------|
| | Model with Injection Ratio of 10% | Model with Injection Ratio of 50% |
| 0.1 | 94.34% | 98.81% |
| 0.01 | 94.04% | 97.61% |
| 0.001 | 86.90% | 95.24% |
| 0.0001 | 80.76% | 93.59% |

found that decreasing the learning rate l for the attack is the only approach that yields meaningful results, *i.e.* producing some scenarios where our detection rate drops below 85%. A small learning rate means the adversary moves more cautiously through the loss landscape to search for adversarial perturbations. As a result, the adversary may find a perturbation associated with an original adversarial example. In the intuition illustrated in Figure 2, a low learning rate along the gradient can find a natural adversarial example.

However, using a higher trapdoor injection ratio (training using more trapdoor images) mitigates against this attack. A higher injection ratio embeds the trapdoor more deeply into the loss landscape of the neural network. This stronger embedding smoothens the manifold, effectively removing other local minima an attacker could previously find using the learning rate attack. Table 6 lists our results on using injection ratio to deal with low learning rate attacks. At a low injection ratio of 10%, detection rate can fall to 80% with an extremely low learning rate of 0.0001. If we adjust the injection ratio up to 50%, *i.e.* use more training samples per trigger, the low learning rate attack is again reliably detected by our trapdoored model. Finally, we note that the low learning rate is accompanied by a proportional increase in computational cost (# of iterations). At some point, the geometric increase in search time will become prohibitively large for practical attacks.

6.3 Adaptive Attacks by Oracle Attackers

The oracle attacker knows everything about embedded trapdoors, including the exact shape and intensity of the trapdoor. These powerful adversaries set the lower bound of our detection robustness.

With knowledge of the embedded trapdoor, the oracle attacker can try to evade trapdoor-enabled detection by jointly minimizing the loss of the adversarial example and the probability that example is detected. The attacker knows the defender uses cosine similarity of a random set of neuron activations to detect adversarial examples. Since attackers do not know the exact neurons selected for each image, they can only approximate it by arbitrarily selecting a set of neuron activations. From there, the attacker needs to minimize the cosine similarity between the selected neuron activation pattern of their attack perturbation and the known trapdoor perturbation. Mathematically, this joint attack loss function can be written as:

$$\min_{\eta} ||\eta||_p + c \cdot \ell(y_t, \mathcal{F}_{\theta}(x + \eta)) + \alpha \cdot \cos(h_N(\eta + x), h_N(Tr_t + x)) \quad (6)$$

where $\cos(\cdot)$ represents the cosine similarity function between two matrices, and h_N is the set of neuron activations selected by the attacker. Note that the defender randomly selects a set of neurons at inference time to compute the neuron signature.

We evaluate the effectiveness of this attack using CW attack with the updated loss function. We targeted the GTSRB model trained in Section 4.2. Even with perfect knowledge of the embedded trapdoor, detection success at 5% FPR only drops to 76.59%. At the same time, L_2 norm of the adversarial perturbations increases by 6.3x. We conclude that the oracle attackers have limited effectiveness (18.84% drop in detection accuracy) against our trapdoor-enabled detection method.

7 Conclusion and Future Work

This paper introduces *trapdoor-enabled detection* of adversarial examples. Our proposed method uses backdoor (a.k.a. Trojan) attacks to create trapdoors that introduce controlled vulnerabilities (traps) into the model. These trapdoors can be injected into the model to defend all labels or particular labels of interest. For multiple application domains, a trapdoor-based defense has high detection success against adversarial examples generated by all the major attacks, including CW, ElasticNet, PGD, BPDA, FGSM, and SPSA, with negligible impact on classification accuracy of normal inputs.

We include discussions and evaluate trapdoors against multiple strong adaptive attacks, including a learning rate attack and an oracle optimization attack. Even when the attacker is able to tolerate very high computation costs and extremely large perturbations, trapdoors remain generally robust with detection above 75%. Finally, while this paper focuses on white box attack scenarios, we refer interested readers to the appendix for strong results on detecting black box attacks.

References

- [1] ATHALYE, A., CARLINI, N., AND WAGNER, D. Obfuscated gradients give a false sense of security: Circumventing defenses to adversarial examples. In *Proc. of ICML* (2018).
- [2] BUCKMAN, J., ROY, A., RAFFEL, C., AND GOODFELLOW, I. Thermometer encoding: One hot way to resist adversarial examples. In *Proc. of ICLR* (2018).
- [3] CAO, Y., YU, A. F., ADAY, A., STAHL, E., MERWINE, J., AND YANG, J. Efficient repair of polluted machine learning systems via causal unlearning. In *Proc. of ASIACCS* (2018).
- [4] CARLINI, N., AND WAGNER, D. Defensive distillation is not robust to adversarial examples. *arXiv preprint arXiv:1607.04311* (2016).
- [5] CARLINI, N., AND WAGNER, D. Adversarial examples are not easily detected: Bypassing ten detection methods. In *Proc. of ACM Workshop on Artificial Intelligence and Security (AISec)* (2017).
- [6] CARLINI, N., AND WAGNER, D. Magnet and efficient defenses against adversarial attacks are not robust to adversarial examples. *arXiv preprint arXiv:1711.08478* (2017).
- [7] CARLINI, N., AND WAGNER, D. Towards evaluating the robustness of neural networks. In *Proc. of IEEE S&P* (2017).
- [8] CHEN, P.-Y., SHARMA, Y., ZHANG, H., YI, J., AND HSIEH, C.-J. Ead: elastic-net attacks to deep neural networks via adversarial examples. In *Proc. of AAAI* (2018).
- [9] CHEN, X., LIU, C., LI, B., LU, K., AND SONG, D. Targeted backdoor attacks on deep learning systems using data poisoning. *arXiv preprint arXiv:1712.05526* (2017).
- [10] CLEMENTS, J., AND LAO, Y. Hardware trojan attacks on neural networks. *arXiv preprint arXiv:1806.05768* (2018).
- [11] DHILLON, G. S., AZIZADENESHELI, K., BERNSTEIN, J. D., KOS-SAIFI, J., KHANNA, A., LIPTON, Z. C., AND ANANDKUMAR, A. Stochastic activation pruning for robust adversarial defense. In *Proc. of ICLR* (2018).
- [12] GOODFELLOW, I. J., SHLENS, J., AND SZEGEDY, C. Explaining and harnessing adversarial examples. *arXiv preprint arXiv:1412.6572* (2014).
- [13] GU, T., DOLAN-GAVITT, B., AND GARG, S. Badnets: Identifying vulnerabilities in the machine learning model supply chain. In *Proc. of Machine Learning and Computer Security Workshop* (2017).
- [14] GUO, C., RANA, M., CISSE, M., AND VAN DER MAATEN, L. Countering adversarial images using input transformations. In *Proc. of ICLR* (2018).
- [15] HE, K., ZHANG, X., REN, S., AND SUN, J. Deep residual learning for image recognition. In *Proc. of CVPR* (2016).
- [16] HE, W., WEI, J., CHEN, X., CARLINI, N., AND SONG, D. Adversarial example defenses: Ensembles of weak defenses are not strong. In *Proc. of WOOT* (2017).
- [17] KINGMA, D. P., AND BA, J. Adam: A method for stochastic optimization. *arXiv preprint arXiv:1412.6980* (2014).
- [18] KRIZHEVSKY, A., AND HINTON, G. Learning multiple layers of features from tiny images. Tech. rep., 2009.
- [19] KURAKIN, A., GOODFELLOW, I., AND BENGIO, S. Adversarial examples in the physical world. *arXiv preprint arXiv:1607.02533* (2016).
- [20] KURAKIN, A., GOODFELLOW, I., AND BENGIO, S. Adversarial machine learning at scale. In *Proc. of ICLR* (2017).
- [21] LIU, Y., MA, S., AAFER, Y., LEE, W.-C., ZHAI, J., WANG, W., AND ZHANG, X. Trojaning attack on neural networks. In *Proc. of NDSS* (2018).
- [22] MA, S., LIU, Y., TAO, G., LEE, W.-C., AND ZHANG, X. Nic: Detecting adversarial samples with neural network invariant checking. In *Proc. of NDSS* (2019).
- [23] MA, X., LI, B., WANG, Y., ERFANI, S. M., WIJEWICKREMA, S., SCHOENEBECK, G., SONG, D., HOULE, M. E., AND BAILEY, J. Characterizing adversarial subspaces using local intrinsic dimensionality. In *Proc. of ICLR* (2018).
- [24] MADRY, A., MAKELOV, A., SCHMIDT, L., TSIPRAS, D., AND VLADU, A. Towards deep learning models resistant to adversarial attacks. In *Proc. of ICLR* (2018).
- [25] MENG, D., AND CHEN, H. Magnet: a two-pronged defense against adversarial examples. In *Proc. of CCS* (2017).
- [26] PAPERNOT, N., MCDANIEL, P., GOODFELLOW, I., JHA, S., CELIK, Z. B., AND SWAMI, A. Practical black-box attacks against machine learning. In *Proc. of AsiaCCS* (2017).
- [27] PAPERNOT, N., MCDANIEL, P., WU, X., JHA, S., AND SWAMI, A. Distillation as a defense to adversarial perturbations against deep neural networks. In *Proc. of IEEE S&P* (2016).
- [28] SAMANGOUËL, P., KABKAB, M., AND CHELLAPPA, R. Defensegan: Protecting classifiers against adversarial attacks using generative models. In *Proc. of ICLR* (2018).
- [29] SHARIF, M., BHAGAVATULA, S., BAUER, L., AND REITER, M. K. Accessorize to a crime: Real and stealthy attacks on state-of-the-art face recognition. In *Proc. of CCS* (2016).
- [30] SONG, Y., KIM, T., NOWOZIN, S., ERMON, S., AND KUSHMAN, N. Pixeldefend: Leveraging generative models to understand and defend against adversarial examples. In *Proc. of ICLR* (2018).
- [31] SPALL, J. C., ET AL. Multivariate stochastic approximation using a simultaneous perturbation gradient approximation. *IEEE transactions on automatic control* 37, 3 (1992), 332–341.
- [32] STALLKAMP, J., SCHLIPSING, M., SALMEN, J., AND IGEL, C. Man vs. computer: Benchmarking machine learning algorithms for traffic sign recognition. *Neural Networks* (2012).
- [33] SUN, Y., WANG, X., AND TANG, X. Deep learning face representation from predicting 10,000 classes. In *Proc. of CVPR* (2014).
- [34] SZEGEDY, C., ZAREMBA, W., SUTSKEVER, I., BRUNA, J., ERHAN, D., GOODFELLOW, I., AND FERGUS, R. Intriguing properties of neural networks. In *Proc. of ICLR* (2014).
- [35] UESATO, J., O'DONOGHUE, B., OORD, A. V. D., AND KOHLI, P. Adversarial risk and the dangers of evaluating against weak attacks. *arXiv preprint arXiv:1802.05666* (2018).
- [36] WANG, B., YAO, Y., SHAN, S., LI, H., VISWANATH, B., ZHENG, H., AND ZHAO, B. Y. Neural cleanse: Identifying and mitigating backdoor attacks in neural networks. In *Proc. of IEEE S&P* (2019).
- [37] XIE, C., WANG, J., ZHANG, Z., REN, Z., AND YUILLE, A. Mitigating adversarial effects through randomization. In *Proc. of ICLR* (2018).
- [38] XU, W., EVANS, D., AND QI, Y. Feature squeezing: Detecting adversarial examples in deep neural networks. In *Proc. of NDSS* (2018).
- [39] <https://www.cs.tau.ac.il/~wolf/ytfaces/>. YouTube Faces DB.
- [40] ZANTEDESCHI, V., NICOLAE, M.-I., AND RAWAT, A. Efficient defenses against adversarial attacks. In *Proc. of ACM Workshop on Artificial Intelligence and Security (AISec)* (2017).
- [41] ZHENG, S., SONG, Y., LEUNG, T., AND GOODFELLOW, I. Improving the robustness of deep neural networks via stability training. In *Proc. of CVPR* (2016).

Table 7: Detailed information about dataset, complexity, and model architecture of each task.

| Task | Dataset | # of Labels | Input Size | # of Training Images | Model Architecture |
|--------------------------|--------------|-------------|-------------------------|----------------------|----------------------------|
| Traffic Sign Recognition | GTSRB | 43 | $32 \times 32 \times 3$ | 35,288 | 6 Conv + 2 Dense |
| Image Recognition | CIFAR 10 | 10 | $32 \times 32 \times 3$ | 50,000 | 20 Residual + 1 Dense |
| Face Recognition | YouTube Face | 1,283 | $55 \times 47 \times 3$ | 375,645 | 4 Conv + 1 Merge + 1 Dense |

Appendix

Experiment Configuration

Model Architecture. We present the architecture of DNN models used in our work.

GTSRB (Table 8) is a convolutional neural network consisting of three pairs of convolutional layers connected by max pooling layers, followed by two fully connected layers.

YouTube Face (Table 9) is the DeepID model trained on the YouTube Face dataset. It has three convolutional layers (connected by pooling layers) followed by three fully connected layers.

CIFAR10 (Table 10) is also a convolutional network but includes 21 sequential convolutional layers, followed by pooling, dropout, and fully connected layers.

Table 8: Model Architecture of GTSRB.

| Layer Type | # of Channels | Filter Size | Stride | Activation |
|------------|---------------|--------------|--------|------------|
| Conv | 32 | 3×3 | 1 | ReLU |
| Conv | 32 | 3×3 | 1 | ReLU |
| MaxPool | 32 | 2×2 | 2 | - |
| Conv | 64 | 3×3 | 1 | ReLU |
| Conv | 64 | 3×3 | 1 | ReLU |
| MaxPool | 64 | 2×2 | 2 | - |
| Conv | 128 | 3×3 | 1 | ReLU |
| Conv | 128 | 3×3 | 1 | ReLU |
| MaxPool | 128 | 2×2 | 2 | - |
| FC | 512 | - | - | ReLU |
| FC | 43 | - | - | Softmax |

Table 9: DeepID Model Architecture for YouTube Face.

| Layer Name (Type) | # of Channels | Filter Size | Stride | Activation | Connected to |
|-------------------|---------------|--------------|--------|------------|--------------|
| conv_1 (Conv) | 20 | 4×4 | 2 | ReLU | |
| pool_1 (MaxPool) | | 2×2 | 2 | - | conv_1 |
| conv_2 (Conv) | 40 | 3×3 | 2 | ReLU | pool_1 |
| pool_2 (MaxPool) | | 2×2 | 2 | - | conv_2 |
| conv_3 (Conv) | 60 | 3×3 | 2 | ReLU | pool_2 |
| pool_3 (MaxPool) | | 2×2 | 2 | - | conv_3 |
| fc_1 (FC) | 160 | - | - | - | pool_3 |
| conv_4 (Conv) | 80 | 2×2 | 1 | ReLU | pool_3 |
| fc_2 (FC) | 160 | - | - | - | conv_4 |
| add_1 (Add) | - | - | - | ReLU | fc_1, fc_2 |
| fc_3 (FC) | 1280 | - | - | Softmax | add_1 |

Model Training and Attack Configurations. Table 11 lists the training specifications for the trapdoored versions of the GTSRB, CIFAR10, and YouTube Face models. Table 12 lists the configurations for each adversarial attack evaluated against our defense. Each attack was tuned to achieve $> 90\%$ success rate against clean models (without any trapdoor).

Table 10: ResNet20 Model Architecture for CIFAR10.

| Layer Name (type) | # of Channels | Activation | Connected to |
|---------------------|---------------|------------|--------------|
| conv_1 (Conv) | 16 | ReLU | - |
| conv_2 (Conv) | 16 | ReLU | conv_1 |
| conv_3 (Conv) | 16 | ReLU | pool_2 |
| conv_4 (Conv) | 16 | ReLU | conv_3 |
| conv_5 (Conv) | 16 | ReLU | conv_4 |
| conv_6 (Conv) | 16 | ReLU | conv_5 |
| conv_7 (Conv) | 16 | ReLU | conv_6 |
| conv_8 (Conv) | 32 | ReLU | conv_7 |
| conv_9 (Conv) | 32 | ReLU | conv_8 |
| conv_10 (Conv) | 32 | ReLU | conv_9 |
| conv_11 (Conv) | 32 | ReLU | conv_10 |
| conv_12 (Conv) | 32 | ReLU | conv_11 |
| conv_13 (Conv) | 32 | ReLU | conv_12 |
| conv_14 (Conv) | 32 | ReLU | conv_13 |
| conv_15 (Conv) | 64 | ReLU | conv_14 |
| conv_16 (Conv) | 64 | ReLU | conv_15 |
| conv_17 (Conv) | 64 | ReLU | conv_16 |
| conv_18 (Conv) | 64 | ReLU | conv_17 |
| conv_19 (Conv) | 64 | ReLU | conv_18 |
| conv_20 (Conv) | 64 | ReLU | conv_19 |
| conv_21 (Conv) | 64 | ReLU | conv_20 |
| pool_1 (AvgPool) | - | - | conv_21 |
| dropout_1 (Dropout) | - | - | pool_1 |
| fc_ (FC) | - | Softmax | dropout_1 |

FGSM is an exception to this rule, only achieving $\approx 34\%$ attack success rate against clean models.

Sample Trapdoor Images. Figure 9 shows sample images with single label defense trapdoor and that with all label defense trapdoor.

Measurement of the Trapdoor

We explore the properties of trapdoors along several dimensions and evaluate their impact on the adversarial example detection rate. Trapdoor properties explored include the magnitude of the trapdoor perturbation, the location in the image, and the injection ratio. We investigate each property using the same experimental setup: a GTSRB model with a single label defended by a trapdoor.

The magnitude of the trapdoor Tr_i forces a tradeoff between the ease of injection and likelihood of “trapping” adversaries. On one hand, we wish to inject trapdoors that are as small as possible. Because the attacker’s objective is to minimize the attack perturbation, it is easier for them to converge to small trapdoors. On the other hand, if the trapdoor is too small, it is hard for the model to learn the trapdoor distribution during the training process.

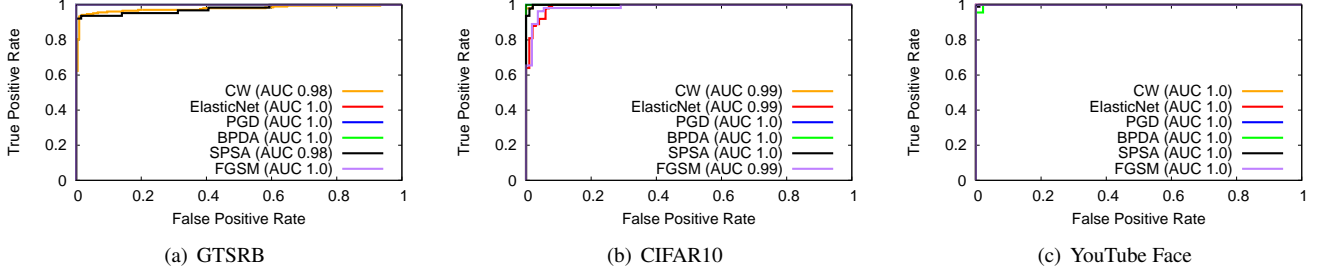


Figure 6: ROC Curve of detection on GTSRB, CIFAR10, YouTube Face with a single label protected by a trapdoor.

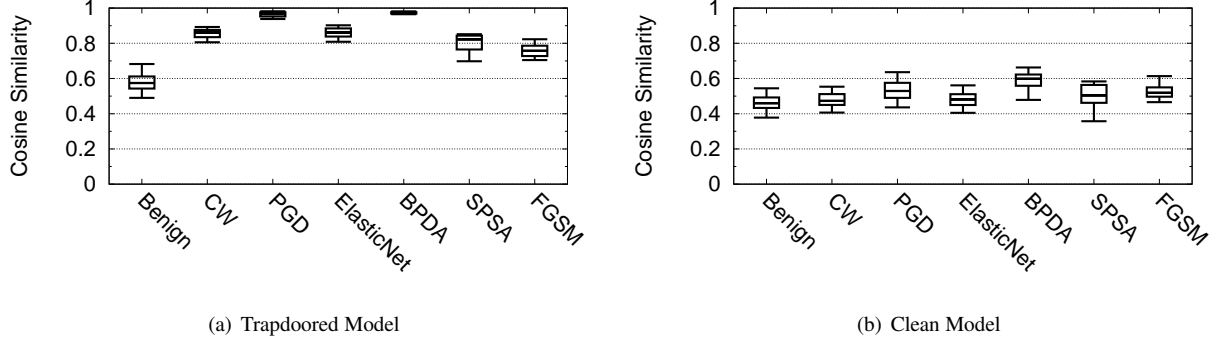


Figure 7: Comparison of cosine similarity of normal images and adversarial images to trapdoored inputs in a trapdoored CIFAR10 model and in a clean CIFAR10 model. The boxes show the inter-quartile range, and the whiskers denote the 5th and 95th percentiles.

We study two ways of changing the $L2$ norm (and thus the magnitude) of the trapdoor: varying the trapdoor size and varying its mask ratio. Both changes minimally impact the detection success rate. Figure 13 shows that when the size of the trapdoor is between 1.5% and 87.9% of the entire image, the detection success rate is higher than 80%. Similarly, when mask ratio is less than 0.3, the detection success at 5% FPR is above 83.34%, as in Figure 14.

The location of the trapdoor also does not impact our detection success. We choose 50 random locations to place the trapdoor. We train a defended model for each trapdoor location. Figure 15 shows that detection success rate is above 80% at 5% FPR for each model.

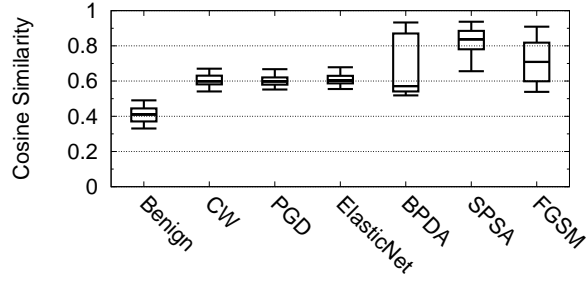
The number of trapdoor images used to train the model does impact the robustness of the trapdoor. We call the percent of trapdoored images present in the training dataset the trapdoor *injection ratio*. A higher injection ratio allows the model to learn the trapdoor better but slightly degrades normal classification accuracy. We defend several models with different trapdoor injection ratios and report the detection success rate in Figure 11. When the injection ratio is less than 3%, the model fails to learn the trapdoor and therefore detection fails. As the injection ratio increases, the normal classification accuracy slowly decreases (a total of 2.75%), as shown in Figure 10.

Black Box Attack. In a black box attack [26], an adversary sends repeated queries a target model, and uses the resulting

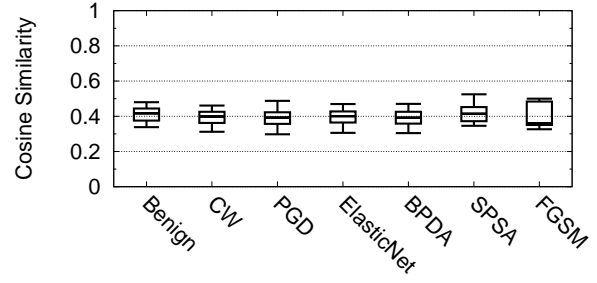
labels to find and map out the classification boundary. Classification results from the target model are then used to train a local substitute model. Finally, adversarial examples are generated using the substitute model, and used to generate misclassifications against the target model.

Black box attacks against a model with embedded trapdoors must walk a fine line. In order to generate meaningful adversarial examples that successfully transfer to the target model, the attacker must try to approximate the target as much as possible. But doing so means that black box attacks can also transfer the trapdoors from the target to the substitute model. To increase the likelihood that a black box attack inherits at least one trapdoor, we use multiple trapdoored defenses in Section 5.1. Moreover, since a black box attacker updates their query inputs by small increments, it is more likely for them to fail into a trap if the trapdoor perturbation is small. Thus, a trapdoor defense with a small mask ratio would be ideal.

We experimentally validate this technique by defending a single label GTSRB model using 100 trapdoors and a mask ratio of 0.05. We construct the substitute model following [26]. Then, we craft attack images on the substitute model, and use them to attack our original model. We observe that the substitute model does indeed inherit the trapdoors, and adversarial examples generated on the substitute model are detected by our trapdoors with an average success rate of 93%. When running trapdoor-enabled detection, we



(a) Trapdoored Model



(b) Clean Model

Figure 8: Comparison of cosine similarity of normal images and adversarial images to trapdoored inputs in a trapdoored YouTube Face model and in a clean YouTube Face model. The boxes show the inter-quartile range, and the whiskers denote the 5th and 95th percentiles.



(a) Single Label Defense Trapdoor (b) All Label Defense Trapdoor

Figure 9: Trapdoor examples used for experiments in Section 4, with mask ratio $\kappa = 1.0$.

are able to detect 100% of all the six attacks at 5% false positive rate.

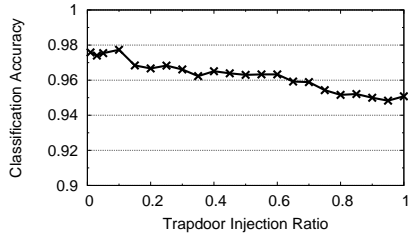


Figure 10: Normal classification accuracy when increasing the injection ratio of the injected trapdoor in GTSRB

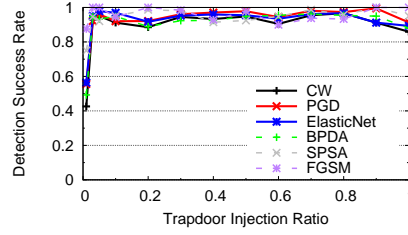


Figure 11: Detection success rate of various adversarial attacks at 5% FPR when increasing the injection ratio of the injected trapdoor in GTSRB.

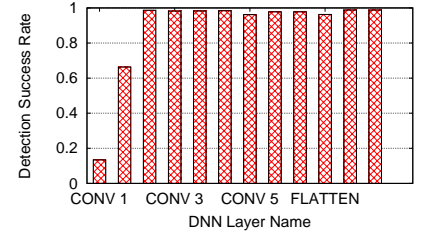


Figure 12: Detection success rate of CW attack at 5% FPR using different layer for detection GTSRB.

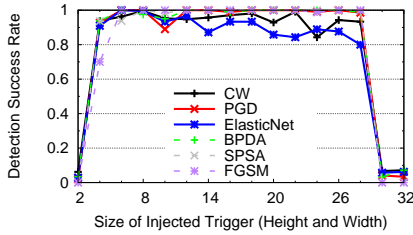


Figure 13: Detection success rate of various adversarial attacks at 5% FPR when increasing the size of the injected trapdoor in GTSRB.

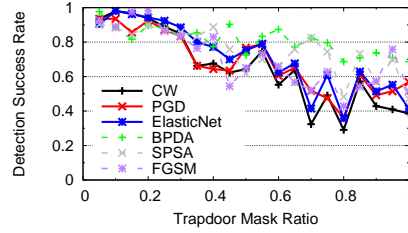


Figure 14: Detection success rate of various adversarial attacks at 5% FPR when increasing the mask ratio of the injected trapdoor in GTSRB.

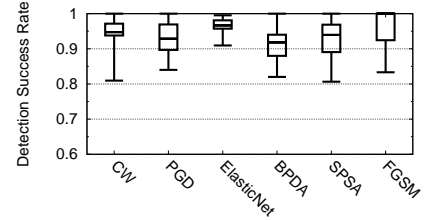


Figure 15: Detection success rate distribution at 5% FPR with differently located trapdoors. Box plot shows min/max and quartiles.

Table 11: Detailed information on datasets and training configurations for each BadNets model.

| Model | # of Labels | Training Set Size | Testing Set Size | Training Configuration |
|--------------|-------------|-------------------|------------------|--|
| GTSRB | 43 | 35,288 | 12,630 | inject-ratio=0.5, epochs=30, batch=32, optimizer=Adam, lr=0.005 |
| CIFAR10 | 10 | 50,000 | 10,000 | inject-ratio=0.5, epochs=100, batch=32, optimizer=Adam, lr=0.005 |
| YouTube Face | 1,283 | 375,645 | 64,150 | inject-ratio=0.5, epochs=30, batch=32, optimizer=Adadelta, lr=1 |

Table 12: Detailed information on attack configurations

| Attack Method | Attack Configuration |
|---------------|---|
| CW | binary step size = 20, max iterations = 500, learning rate = 0.1, abort early = False |
| PGD | max eps = 8, # of iteration = 100, eps of each iteration = 1.0 |
| ElasticNet | binary step size = 20, max iterations = 500, learning rate = 0.5, abort early = False |
| BPDA | max eps = 8, # of iteration = 100, eps of each iteration = 1.0 |
| SPSA | eps = 8, # of iteration = 500, learning rate = 0.1 |
| FGSM | eps = 8 |